OIL SEAL DYNAMICS: CONSIDERATIONS FOR ANALYSIS OF CENTRIFUGAL COMPRESSORS

by

R. Gordon Kirk

Associate Professor

Virginia Polytechnic Institute

and State University

Blacksburg, Virginia

R. Gordon Kirk is Associate Professor of Mechanical Engineering at Virginia Polytechnic Institute and State University in Blacksburg, Virginia. His current research interests are in the area of seal influence on rotor response and stability, bearing and seal analysis and testing for dynamic characteristics, influence of rotor construction on balance, modal testing, and active control of rotor response. He studied Mechanical Engineering at the University of Virginia where he received a B.S. degree with high distinction in 1967, a M.S. degree in 1969, and a Ph.D. degree in 1972.

While working toward his Ph.D., he taught Mechanical Engineering at the University of Virginia, and as a Research Engineer, worked on a NASA contract for transient analysis of flexible rotor-bearing systems. After receiving his Ph.D., he worked for Pratt and Whitney Aircraft in East Hartford, Connecticut, in rotordynamics analysis and transient response analysis.

In 1975, Dr. Kirk joined Ingersoll-Rand as a Senior Analyst in the Development Group, and continued to develop expertise in rotordynamics analysis and investigate the influence of oil seals on the stability of compressor rotors. His work resulted in a patent for a unique bearing support system, and the work on oil seals resulted in a second patent for stabilized-cone oil seals. A third patent was awarded for an optimum fluid film pocket bearing. As Analytical Engineer Group Supervisor for the Turbomachinery Division of Ingersoll-Rand Company, Dr. Kirk was responsible for the rotor-bearing design and analysis of all the Turbomachinery Division compressors, turbines, and hot gas expanders.

Dr. Kirk is the author of more than 35 technical papers and reports on rotor-bearing design and analysis.

ABSTRACT

Oil seals are used in many industrial compressor designs where positive control of the process gas is essential. Consideration of the influence of these seals is necessary for proper design evaluation. The oil seals can have a controlling influence under certain conditions of loading, supply pressure, and rotor speed.

The analysis of the loading and hydrodynamic forces as applied to typical design studies is reviewed. Results of test and field data support the general method of analysis methods and points to future test results needed to fully understand the dynamics of the oil seals and their influence on the stability and response sensitivity of a rotor system.

INTRODUCTION

The current trends in the turbocompressor field are increased design speeds, more stages per casing, higher pressures, increased efficiency, and longer bearing-to-bearing spans. With regard to rotor response, strict attention has been paid to rotor modelling, fluid-film bearing characteristics, and in some instances, the influence of the supporting structure. One very important additional element in high presure compressors is the method of modelling floating-ring oil seals and the determination of their influence on rotor response and dynamic stability.

For compressors that have design speed below twice the first flexural critical, the chances of having nonsynchronous whirl (shaft whip) are small for machines that utilize tilting-pad type bearings. When the design speed is in excess of twice the first critical speed, the design engineer must be aware of the potential of nonsynchronous whirl. A shaft whip instability may be generated as the result of fixed geometry bearing design, aerodynamic excitation, internal friction of shrink fits and built-up rotors, labyrinth seals, or oil seal dynamic interaction with the rotor bearing system.

Black [1, 2] has documented the analysis of high-axial-flow seals (Reynolds number > 2000) which is applicable for small clearance, high-pressure water seals, but not the lower Reynolds number axial flow typical of turbo-compresor oil seals. The analysis of high pressure oil seals will be reviewed and updated [3].

Further extension of the original analysis [3] incorporated a thermal heat balance [4] for the oil seal ring(s). These equations are reviewed as the global heat balance procedure is explained for basic analysis calculations. The method of calculating the operating eccentricity of a single breakdown seal cartridge is presented in detail. With the operating eccentricity, average film temperature, and pressure distribution known, the stiffness and damping characteristics may be calculated for the eccentric oil seal ring.

The limitations of the analysis capabilities and recommendations for future analysis and testing required to fully understand the dynamic operation of oil-seal rings and their influence on the dynamic stability of high speed, high pressure, flexible shaft turbocompressors will be discussed.

ANALYSIS OF OIL SEAL RINGS

Overall Operation

The cross section of a typical single breakdown oil seal is shown in Figure 1. The seal cartridge contains two elements loaded by a series of springs to assist in initial asembly and pressurization of the seals. The seal oil presure is maintained at suction (P_s) plus an increment (ΔP) which is typically generated by overhead oil supply tanks. The inner seal, thus, has a drop of ΔP, whereas the outer seal has a drop from $P_s + \Delta P$ to outer drain pressure, P_o.
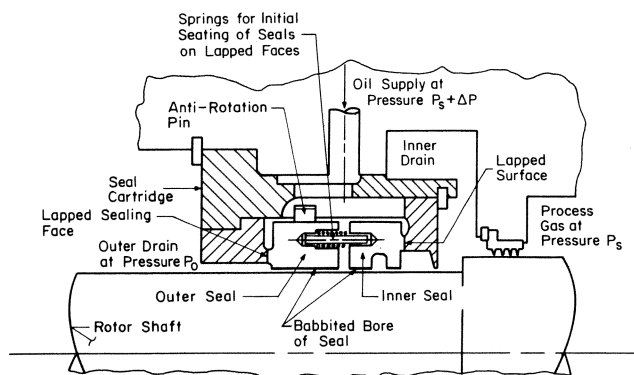
25

Figure 1. Typical Oil Seal Configuration.

An antirotation pin is typically provided for each of the outer seal rings. The external radial loading from the pin has been assumed to be negligible as compared to the friction loading from the seal ring-retainer interface.

Theory of Hydrodynamic oil film

The seal rings are actually floating bearing elements that, when locked, generate the full hydrodynamic fluid-film reaction. To establish a model of the fluid-film interface, the solution of the general Reynolds' equation will be considered. The governing equation is then [5]:

$$\frac{\partial}{\partial z}\left[\frac{h^3}{6\mu}\frac{\partial P}{\partial z}\right] + \frac{1}{R^2}\frac{\partial}{\partial \theta}\left[\frac{h^3}{6\mu}\frac{\partial P}{\partial \theta}\right] = \omega\frac{\partial h}{\partial \theta} + 2\frac{\partial h}{\partial t} \quad (1)$$

The local film thickness can be expressed in fixed coordinates by the following equations:

$$h = c - x\,COS\theta - y\,SIN\theta \quad (2)$$

where

θ = angle measured from the positive x-axis in the direction of rotation

c = seal radial clearance

x,y = relative displacement of seal ring with respect to the rotor.

Oil seal rings typically have L/D values that range from $0.05 \le L/D \le 0.2$. Hence, the solution technique will take advantage of short bearing theory [5, 6] and neglect the $\partial P/\partial \theta$ term in Equation (1). The resulting hydrodynamic pressure can then be expressed in fixed x,y coordinates as:

$$P(\theta, z) = \frac{3\mu z(z-L)}{h^3}\left[\omega(x\,SIN\theta - y\,COS\theta)\right.$$

$$\left. - 2(\dot{x}\,COS\theta + \dot{y}\,SIN\theta)\right] \quad (3)$$

The static pressure (i.e., the pressure field which, when added to the hydrodynamic pressure, gives the resultant instantaneous pressure field) is assumed to be a linear drop to suction or outer drain pressure. This is expressed as follows for the outer seal ring:

$$P_{static} = P_o + \frac{z}{L}(P_s + \Delta P - P_o) \quad (4)$$

The components of force on the shaft may be found by integrating the total pressure field around the shaft. This is expressed as.

$$F_{ffx} = \int_{z=0}^{L}\int_{\theta=0}^{2\pi}(P(\theta,z) + P_{static})\,R\,COS\theta\,d\theta\,dz \quad (5)$$

$$F_{ffy} = \int_{z=0}^{L}\int_{\theta=0}^{2\pi}(P(\theta,z) + P_{static})\,R\,SIN\theta\,d\theta\,dz \quad (6)$$

The static pressure field is included, since this controls the cavitation boundary. The integrals may be evaluated by application of numerical integration. A seven point, Weddles Rule, integration has been used for the results presented.

For the condition that the static pressure field is negligible, or when it is greater than the largest negative hydrodynamic pressure level, the z dependence may be integrated to give:

$$\left\{\frac{F_{ffx}}{F_{ffy}}\right\} = \frac{\mu RL^3}{2}\int_{\theta=0}^{2\pi}$$

$$\frac{\omega(x\,SIN\theta - y\,COS\theta) - 2(\dot{x}\,COS\theta + \dot{y}\,SIN\theta)}{(c - x\,COS\theta - y\,SIN\theta)^3}\left\{\frac{COS\theta}{SIN\theta}\right\}d\theta \quad (7)$$

This expression is valid for either a π or 2π film and is only approximate when the pressure field has cavitation which does not extend over a π film. The load capacities for these limiting conditions are shown in Figure 2, where the modified Sommerfeld number is plotted vs eccentricity. Typical oil seal load capacities tend to fall very near the noncavitating curve. The oil film has a load capacity expressed by:

$$S_s = \frac{(1-\epsilon^2)^{3/2}}{2\pi^2\epsilon}\ldots\text{Non-Cavitated} \quad (8a)$$

$$S_s = \frac{(1-\epsilon^2)^2}{\pi\epsilon\sqrt{\pi^2(1-\epsilon^2) + 16\,\epsilon^2}}\ldots\text{Cavitated} \quad (8b)$$
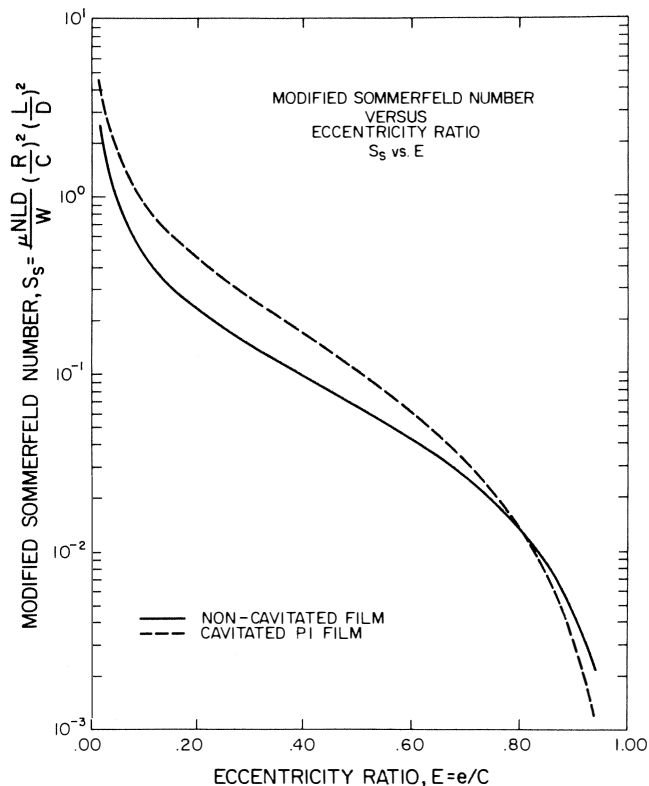

Figure 2. Modified Sommerfeld Number vs Eccentricity for Oil Seals.

The stiffness and damping properties of the oil seal rings are expresed as [3, 5]:

$$K_{xx} = -\frac{\mu RL^3 \omega}{2c^3}$$

$$\int_0^{2\pi} \frac{SIN\theta COS\theta H + 3COS^2\theta(XSIN\theta - YCOS\theta)}{H^4} d\theta \quad (9)$$

$$K_{yy} = \frac{-\mu RL^3 \omega}{2c^3}$$

$$\int_0^{2\pi} \frac{3SIN^2\theta(XSIN\theta - YCOS\theta) - SIN\theta COS\theta H}{H^4} d\theta \quad (10)$$

$$K_{xy} = \frac{-\mu RL^3 \omega}{2c^3}$$

$$\int_0^{2\pi} \frac{3SIN\theta COS\theta(XSIN\theta - YCOS\theta) - HCOS^2\theta}{H^4} d\theta \quad (11)$$

$$K_{yx} = \frac{-\mu RL^3 \omega}{2c^3}$$

$$\int_0^{2\pi} \frac{3SIN\theta COS\theta(XSIN\theta - YCOS\theta) + HSIN^2\theta}{H^4} d\theta \quad (12)$$

$$C_{xx} = \frac{\mu RL^3}{2c^3} \int_0^{2\pi} \frac{2COS^2\theta}{H^3} d\theta \quad (13)$$

$$C_{yy} = \frac{\mu RL^3}{2c^3} \int_0^{2\pi} \frac{2SIN^2\theta}{H^3} d\theta \quad (14)$$

$$C_{xy} = \frac{\mu RL^3}{2c^3} \int_0^{2\pi} \frac{2SIN\theta COS\theta}{H^3} d\theta \quad (15)$$

$$C_{yx} = C_{xy} \quad (16)$$

where

$$H = \frac{h}{c} = 1 - X COS\theta - Y SIN\theta \quad (17)$$

$$X = \frac{x}{c}; \quad Y = \frac{y}{c} \quad (18)$$

The solution of the seal equilibrium position is a very complicated procedure, due to the frictional drag loading from the sealing faces. The seal attitude angle as a function of eccentricity is, therefore, indeterminate. The stiffness and damping properties for a noncavitating oil seal ring are given in Figure 3 for an attitude angle of 90 degrees as a function of Sommerfeld number, and the results for an attitude angle of 135 degrees are shown in Figure 4. It is noted that a destabilizing cross-coupled stiffness, in addition to positive damping terms is generated in the locked seal element.

Force Balance on Inner and Outer Seal Rings

The pressure drop per outer seal ring is typically on the order of 130 to 260 $N-cm^{-2}$ with the incremental pressure ΔP, adjusted to be approximately 4.8 $N-cm^{-2}$. Neglecting en-

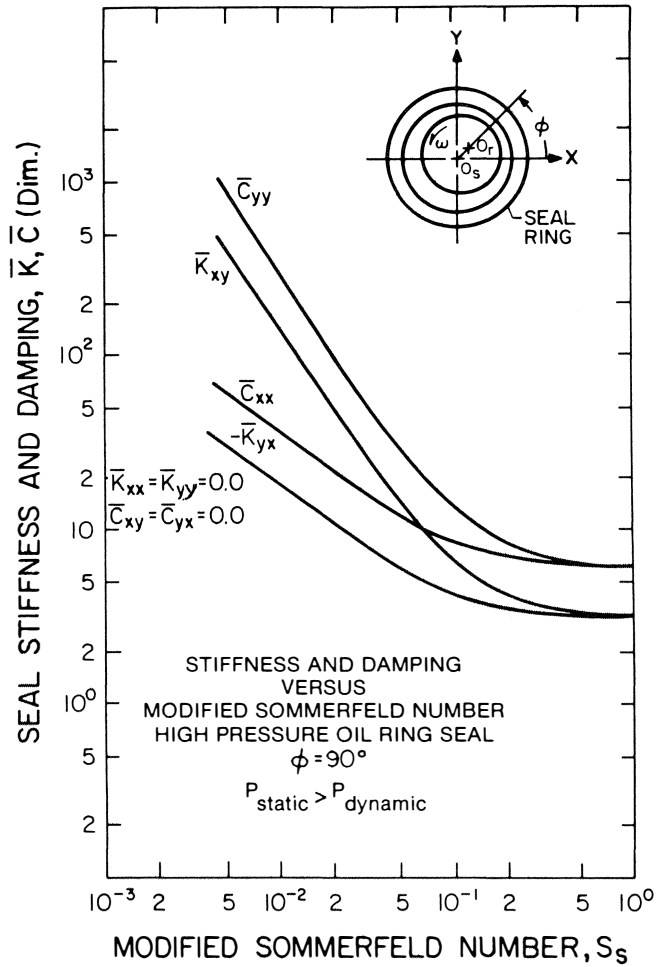*Figure 3. Stiffness and Damping Properties for High Pressure Oil Seals* $\phi = 90°$.

trance effects on the axial flow, the global Reynolds number typically indicates no turbulence corrections are required. For a 260 $N-cm^{-2}$ drop across a typical seal element, the Reynolds number for axial and circumferential flows are:

$$Re_z = \frac{2Vc}{\nu} = 144.3 \quad (19a)$$

$$Re_\theta = \frac{Rc\omega}{\nu} = 524.6 \quad (19b)$$

The method of solution lends itself to local correction on viscosity for turbulence effects when required. The correction may be incorporated into the solution in terms of a modified local viscosity. The local Reynolds number is expressed as:

$$Re_L = \rho Rh\omega/\mu \quad (19c)$$

The modified local viscosity may then be expresed as [7]:

$$\mu_{eff} = j\mu = 1.0139 \ Re^{0.657}\mu \quad (20a)$$

with the restriction that $j \geq 1.0$.

The influence of high pressure on the viscosity of the oil must also be accounted for when the pressures are in excess of 345 $N-cm^{-2}$ (500 psi). Fuller [9] expressed this factor as:
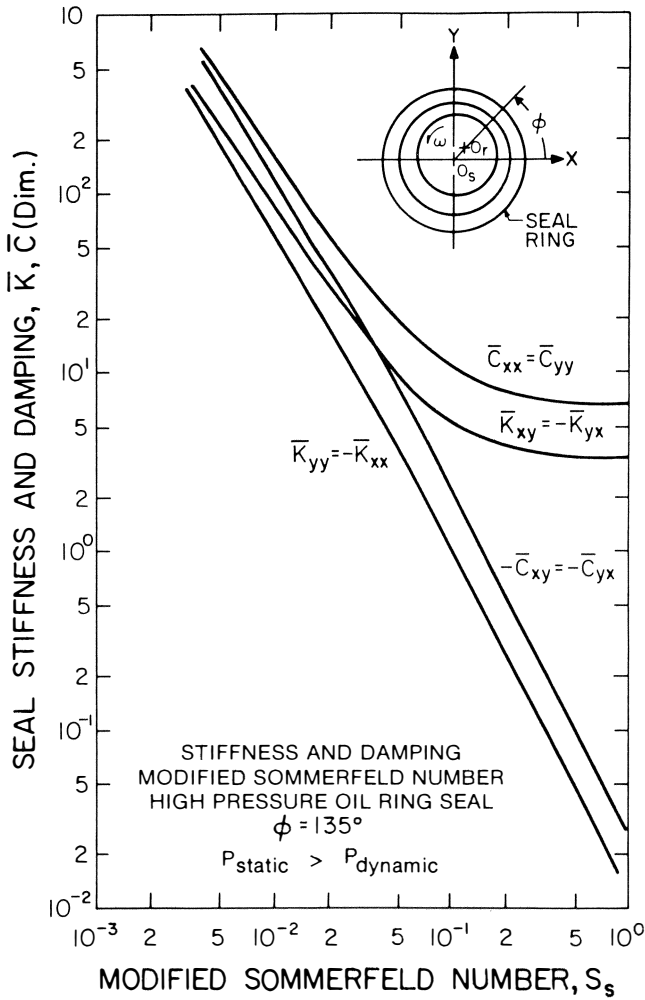
$$\mu_{eff} \mid_p = \mu_{eff} \ e^{Bp} \quad (20b)$$

Figure 4. Stiffness and Damping Properties for High Pressure Oil Seals φ = 135°.

For light turbine oil, the value of B is given as 1.37×10^{-4} in^2lb^{-1}. This value of B gives a 1.07 correction factor for a pressure of 345 Ncm^{-2} (500 psi). Considering the inner seal and referring to Figure 5, the force balance can be expressed in terms of the seal geometry and the oil-supply-pressure level. The relatively small pressure drop across the inner seal produces a low normal loading on that seal ring in the axial direction. A linear pressure gradient $\partial P/\partial r$ is usually assumed across the seal lip interface. The inner seal ring, axial-thrust-load equation, including the spring load, may be expressed as:

$$F_{N_i} = F_s + \frac{\pi}{4}(D_{o_i}^2 - D_{i_i}^2)\, \Delta P \beta_{F_i} + \frac{\pi}{4}\,(D_{i_i}^2 - D_{s_i}^2)\, \Delta P \qquad (21)$$

The parameter β_F is a function of the condition of the lapped sealing surface. The calculation of β_F for an assumed linear pressure drop across the lapped face is given in the Appendix. The axial-thrust load is multiplied by the appropriate coefficient of friction which yields the resisting friction force.

$$F_{\mu_i} = \mu_i F_{N_i} \qquad (22)$$

The coefficient of friction is a function of surface finish, pressure loading, and the boundary lubrication conditions at the lapped seal lip-retainer interface. The resultant external seal radial loading is the vector sum of the friction load, which acts in
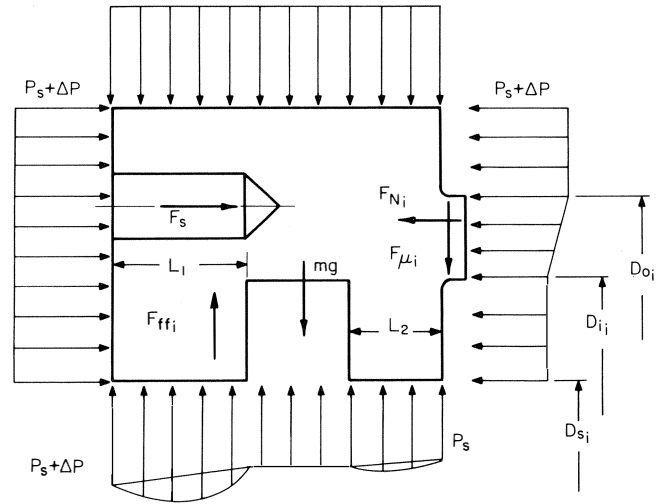

Figure 5. Force Balance for a Typical Inner Seal Ring.

direction opposite that of the seal ring velocity, and the inner seal weight. This is expressed as:

$$F_{x_i} = \vec{F}_{\mu_i} \cdot \vec{\eta}_{x_i} \qquad (23)$$

$$F_{y_i} = \vec{F}_{\mu_i} \cdot \vec{\eta}_{y_i} - M_{s_i}g \qquad (24)$$

where

$$(\vec{\eta}_x, \vec{\eta}_y) = \left(\frac{-\dot{X}}{\sqrt{\dot{X}^2 + \dot{Y}^2}}, \frac{-\dot{Y}}{\sqrt{\dot{X}^2 + \dot{Y}^2}} \right) \qquad (25)$$

A similar analysis can be performed for the outer seal ring. The pressure drop across this ring is large, which gives rise to a high normal loading. The mating surfaces of the seal ring and the retaining ring are finely lapped surfaces which are assumed to give a nearly perfect seal. The pressure between the seal-ring lip and the stationary retaining ring is assumed to be linear based on current knowledge of seal dynamic forces. The actual pressure is not known, due to the thermal and mechanical distortion of the end plate at design conditions. A factor β_{F_o}, ranging from $0 \rightarrow 1.0$ is therefore specified for a particular design. A force balance yields (Figure 6):

$$F_{N_o} = F_s + \{\frac{\pi}{4}(D_{o_o}^2 - D_{i_o}^2)\, \beta_{F_o} + \frac{\pi}{4}\,(D_{i_o}^2 - D_{s_o}^2)\}(P_s + \Delta P - P_o) \qquad (26)$$
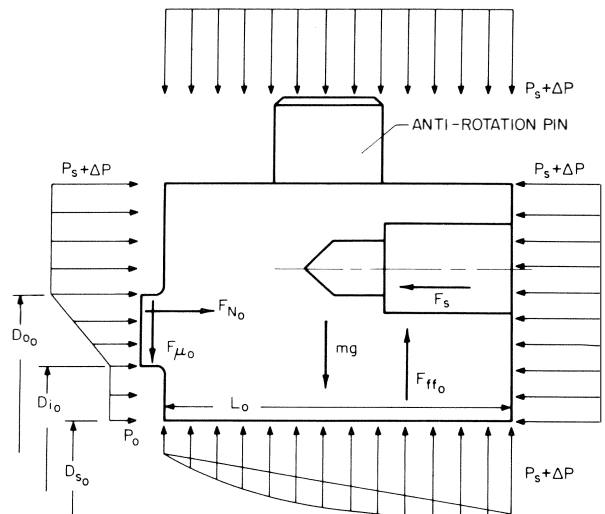

Figure 6. Force Balance for a Typical Outer Seal Ring.

The outer-seal-ring axial load is multiplied by the coefficient of friction which yields the resisting friction force. The resultant, external, outer-seal loading is expressed in component form as:

$$F_{x_o} = \vec{F}_{\mu_o} \cdot \vec{\eta}_{x_o} \tag{27}$$

$$F_{y_o} = \vec{F}_{\mu_o} \cdot \vec{\eta}_{y_o} - M_{s_o}g \tag{28}$$

Example No. 1

The design of an oil-seal ring should consider the variation of the many design parameter. For example, calculate the influence of β_{F_o} on seal loading dimensions given by the following typical values:

$$
\begin{array}{lll}
D_S & = 12.715 \text{ cm} & (5.006 \text{ in}) \\
D_i & = 13.97 \text{ cm} & (5.5 \text{ in}) \\
D_o & = 15.24 \text{ cm} & (6.0 \text{ in}) \\
P_S + \Delta P & = 344.8 \text{ N cm}^{-2} & (500 \text{ lb}_f \text{in}^{-2})
\end{array}
$$

The pressure loading for a perfect seal at the lapped surface outer diameter is:

$$F_P = \frac{\pi}{4}(D_i^2 - D_S^2)[500] + \frac{\pi}{4}(D_o^2 - D_i)\beta_F(500)$$

$$= \frac{\pi}{4}(5.5^2 - 5.006^2)[500] + \frac{\pi}{4}(6^2 - 5.5^2)\, 500\,\beta_{F_o}$$

and with the sealing point at D_o, then

$$\beta_{F_o} = 1.0$$

and

$$F_{P_o}\Big|_{\beta_F = 1} = 2038 + 2258 = 4296 \text{ lb}_f \,.$$

With the seal perfect at the inner lapped surface diameter, $\beta_{F_o} = 0$, and the axial loading is given by the following result:

$$F_P\Big|_{\beta_F = 0} = 2038 \text{ lb}_f \,.$$

Clearly, the pressure distribution is of great concern for both static and dynamic analyses, since the loading can vary by more than a factor of two. This in turn influences the predicted seal locking eccentricity.

The steady state seal equilibrium eccentricity may be found for either the outer or inner seal by utilization of the seal capacity curve shown in Figure 2. Assuming the seal weight to add to the resultant friction load, as a worst case, the maximum seal eccentricity may be calculated. The seal capacity is expressed as:

$$S_s = \frac{\mu\omega LD}{2\pi(F_\mu + M_s g)}\left(\frac{R}{c}\right)^2\left(\frac{L}{D}\right)^2 \tag{29}$$

The actual equilibrium eccentricity is then bounded by the two curves in Figure 2. Typical seal configurations have consistently given results that fall very close to the noncavitating curve.

Analysis of Steady-State Thermal Equilibrium

The solution procedure consists of the calculation of the seal-ring frictional load which is a function of the pressure differential, geometry of the sealing ring, the coefficient of friction of the lapped radial sealing face, and the spring loading.

$$W = f(\Delta P, \mu_f, D_o, D_i, D_s, F_N) \tag{30}$$

With this loading information, Equation (8) may now be solved for the operating eccentricity ratio, ϵ, for an assumed oil viscosity, μ_o. The solution then requires a thermal-flow equilibrium.

The axial flow may be calculated from:

$$Q = Q_o(1 + 1.5\,\epsilon^2) + Q_H(\delta) \tag{31}$$

where

Q_o = non-rotating centered seal axial pressure flow
$$= \Delta P\,\pi\,D\,c^3/(12\mu L) \tag{32}$$
Q_H = hydrodynamic positive end leakage (7)
$$= (\pi/2)D\,L\,c\,N'\epsilon \tag{33}$$
δ = factor ranging from 0.0 to 1.0 and a function of the zone of cavitation.

Hence,

$$Q = f(\Delta P, D, c, \mu, L, \epsilon, N) \tag{34}$$

The hydrodynamic end leakage is considered to be negligible for the pressure levels usually encountered in this type of sealing design. The hydrodynamic pumping, positive and negative, tends to mix the oil stream and increases the validity of using an average film temperature.

The current solution procedure also assumes that the entrance and exit effects are negligible as compared to the viscous losses in the sealing length. Typical ratios of sealing length to clearance are $50 \leqslant L/c \leqslant 400$. Additionally, the entrance to the seal can be chamfered to reduce entrance losses which further justifies the use of Equation (32).

Example 2

$\Delta P = 100 \text{ psi } (68.9 \text{ N/cm}^2)$; $D = 2.75 \text{ in } (6.99 \text{ c.m}) c = 0.0045 \text{ in } (0.0144 \text{ cm})$; $L = 0.938 \text{ in } (2.383 \text{ cm}) N = 12,000 \text{ cpm} = 200 \text{ rev/sec}$; $\epsilon = 0.5 \mu = 1.0 \times 10^{-6} \text{ reyns } (.689 \text{ N sec/cm}^2)$ The seal axial pressure flow is:

Example 2

$\Delta P = 100 \text{ psi } (68.9 \text{ N/cm}^2)$; $D = 2.75 \text{ in } (6.99 \text{ cm})$
$c = 0.0045 \text{ in } (0.0144 \text{ cm})$; $L = 0.938 \text{ in } (2.383 \text{ cm})$
$N = 12,000 \text{ RPM} = 200 \text{ rev/sec}$; $\epsilon = 0.5$
$\mu = 1.0 \times 10^{-6} \text{ reyns } (.689 \text{ N sec/cm}^2)$

The seal axial pressure flow is

$$Q_{\Delta P} = \frac{100 \times \pi \times 2.75 \times (0.0045)^3}{12 \times 1 \times 10^{-6} \times 0.938}(1 + 1.5(.5)^2)$$

$$= 6.994(1.375) = 9.62 \text{ in}^3/\text{sec } (157.6 \text{ cm}^3/\text{sec})$$

The hydrodynamic end leakage is

$$Q_H = \pi \times 2.75 \times 0.938 \times (0.009) \times \frac{200}{4} \times 0.5 \times \delta$$

$$= 1.82 \text{ in}^3/\text{sec} \times \delta \ (29.8 \text{ cm}^3/\text{sec} \times \delta)$$

The centerline hydrodynamic pressure is given by [6]

$$P = \frac{6\,\mu\,\pi\,N^1}{c^2}\left(\frac{L^2}{4}\right)\left(\frac{\epsilon \sin\theta}{(1 + \epsilon\cos\theta)^3}\right) \tag{35}$$

The peak pressure is therefore less than the following for $\epsilon = 0.5$:

$$P_{max} < \frac{6\mu\pi N'L^2}{4c^2} \, \epsilon = \frac{6\times 1\times 10^{-6}\times \pi \times 200 \times 0.938^2 \times 0.5}{4\times(0.0045)^2}$$

$$= 20.47 \text{ lb/in}^2 \ (14.11 \text{ N/cm}^2)$$

Hence, $\delta + 0$ and $Q = Q_{\Delta P}$

The flow is assumed to carry away the heat of the hydrodynamic losses and the extrusion losses. The desired unknown variable is the temperature rise of the oil which is then given by the following equation (specific heat = 0.42):

$$\Delta T = \Delta T|_{hydrodynamic} + \Delta T|_{extrusion}$$

$$\Delta T|_{o_F} = \frac{3.908\times \dfrac{(\dfrac{D\times L\times \mu \times N'}{2.0})^2}{c^4(\Delta P \times \sqrt{1-\epsilon^2}\times(1+1.5\,\epsilon^2))}} + .008 \ \Delta P \tag{36}$$

Now, Equations (8), (30), and (31), and (36) must be solved in an iterative manner to achieve equilibrium of both seal eccentricity and fluid-film average film temperature.

Torque Balance on Seal Rings

The previous analysis has not been concerned with the interaction of the fluid shear torque, the friction torque of the lapped surface, or the anti-rotation pin. A first pass examination of the condition of potential ring spin and resulting damage for the anti-rotation lug will be summarized in this section. The fluid shear torque and resulting moment that could spin the oil ring is given by:

$$M_{film} = \frac{2\pi \mu R^3 \omega \ L/c}{(1-\epsilon^2)^{1/2}} \tag{37}$$

The resisting moment from the axial loading produces a moment at equilibrium of:

$$M_{face} = \frac{\mu N \ LD^2 (R/c)^2 (L/D)^2 \ 2\pi^2 \epsilon}{2(1-\epsilon^2)^{3/2}} \tag{38}$$

These two equations can be solved for the required (L/D) to prevent spin. The result for the non-cavitated seal gives the following design specification to prevent ring spin:

$$\frac{L}{D} > \sqrt{\frac{1-\epsilon^2}{\epsilon}\times(R/c)^{-1}} \tag{39}$$

Example 3

An oil ring having a clearance ratio of 0.002 and an equilibrium eccentricity ratio of $\epsilon = 0.5$ must be modified to stabilize a compressor. What minimum L/D should be specified?

$$\frac{L}{D}_{.002} > \sqrt{\frac{1-.5^2}{.5}(500)^{-1}} = .055$$

If the clearance ratio, C/R, at design temperature is .0015, then

$$\frac{L}{D}_{.0015} > 0.048$$

This example indicates that typical design conditions will require a minimum L/D of approximately 0.05. This magic number has been the basic rule of modified seal design for many years. The origin of the number is not known but the purpose of staying above a give L/D is better understood from the above analysis of the ring-spin torque balance.

CASE HISTORIES OF OIL SEAL RING INFLUENCE ON COMPRESSOR STABILITY

Numerous compressors have been known to exhibit oil seal excited instabilities. The earlier cases were classical examples of a locked ring driving the compressor at the rotor first bending frequency. The results reported [3] are shown in Figures 7 and 8 for a standard design and then a grooved seal design with reduced startup pressure (i.e., a soft start). These results were obtained from actual field conditions, and the absence of the instability under these improved seal loading conditions did produce the desired results.
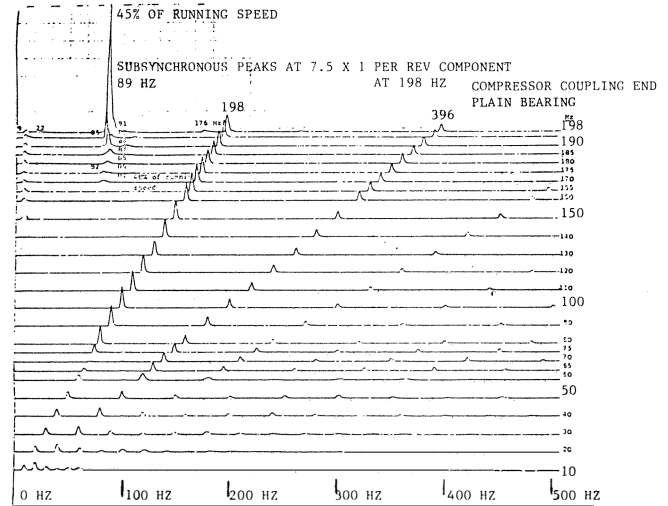

Figure 7. *Frequency Scan for a Multi-Stage Compressor Showing Onset of Seal Induced Shaft Whip near 166 Hz.*
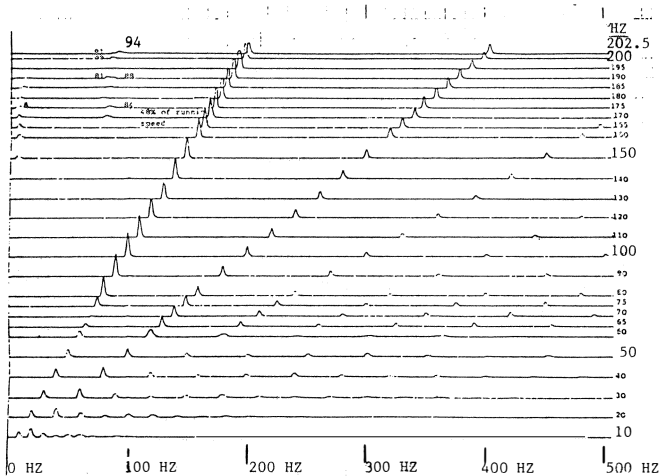

Figure 8. *Frequency Scan for a Multi-Stage Compressor with Startup Pressure Sequence Modified to Assure Oil Seals are Centered Showing Absence of Shaft Whip above 166 Hz.*

Another example of ring seal influence on stability is shown in Figures 9, 10, and 11. The test-stand run with seals as designed shows a strong instability portrayed in Figure 9. With the seal rings removed, the spectrum is clear (Figure 10). When modified seals with circumferential grooving were installed, the acceptable results presented in Figure 11 were obtained. The improvement in stability was the result of modifying the seals. The inverse result on response is illustrated in Figures 12 and 13 where the decrease in damping increases the amplification of the compressor first critical speed under otherwise identical test

conditions. The improvement in stability at higher speeds reduced the positive damping for operation through the critical speed.
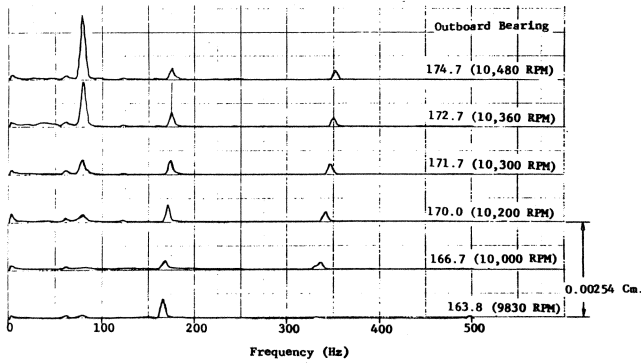

Figure 9. Frequency Scan for a Five-Stage Compressor Showing Onset of Seal Induced Shaft Whip Instability (Outboard Location).
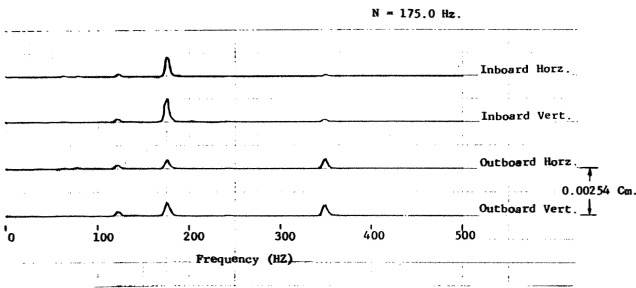

Figure 10. Frequency Scan for a Five-Stage Compressor Showing Total Absence of Shaft Whip at Design When Seal Elements Are Eliminated.
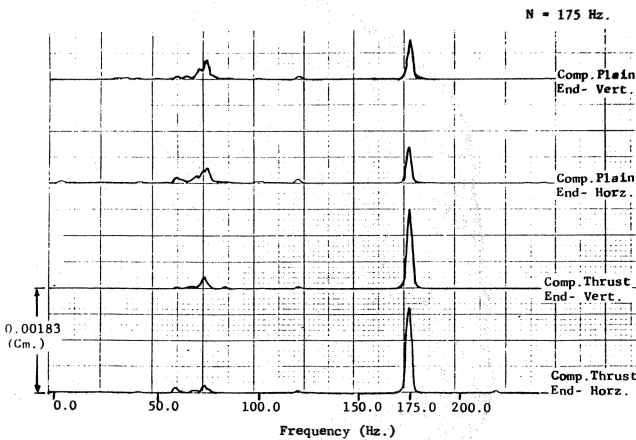

Figure 11. Frequency Scan for a Five-Stage Compressor Having Modified Seal Cartridge Showing Only a Small Component of Nonsynchronous Whirl.

The previous examples illustrate a condition of rotor instability known as shaft whip. It is possible to get the oil seal ring to react at its own resonant frequency. This condition, called seal whip, produces an excitation that can be detected on the rotor radial probes as shown in Figure 14. The seal ring will whip at a low fraction of running speed as shown in the figure and was thought to be solely due to very low axial loading. This compressor was running with only ten psi suction. By increasing the suction pressure to 50 psi, the seal whip vibration was eliminated as shown in Figure 15. Low pressure, centered seals
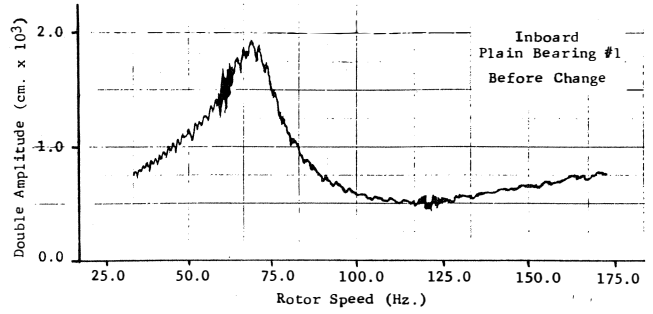

Figure 12. Response of a Five-Stage Compressor before Seal Modification.
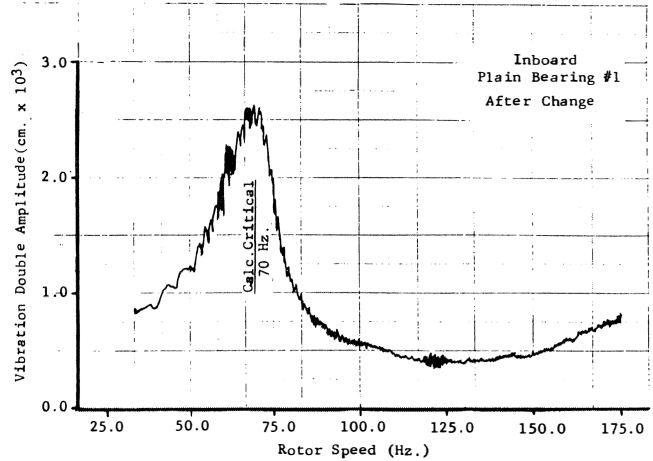

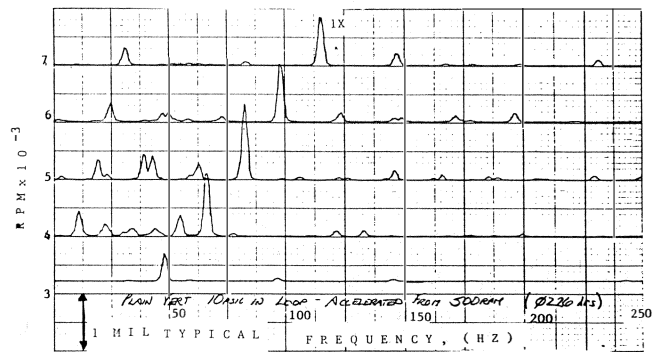Figure 13. Response of a Five-Stage Compressor after Seal Modification.

Figure 14. Frequency Scan for Compressor Having 10 psig Seal Pressure Showing Oil Seal Whip Instability.

were originally thought to be highly desirable, but this case illustrates that a minimum loading is required for total system stability.

Another more recent experience [8] of a similar problem was encountered with a standard cone seal design as shown in Figure 16. Examination of the outer seal ring, after a very short running time, produced damage on the lapped sealing face as illustrated in the photo of Figure 17. The pressure level was not low (70 psi) and stronger seal springs were tried without improvement in the seal damage. A typical response spectrum of the compressor is given in Figure 18, and is noted to be similar to the seal whip condition shown in Figure 14. The seal design was modified, as shown in Figure 19, to improve the compressors stability at design speed. This modification alone was not adequate to solve
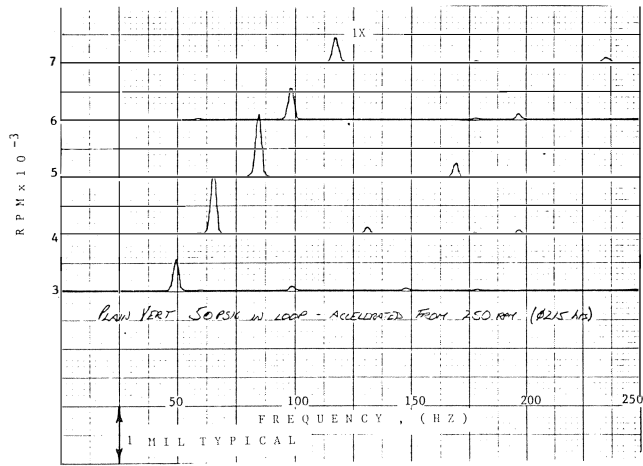
Figure 15. *Frequency Scan for Compressor Having 50 psig Seal Pressure Showing Stable Seal and Rotor System.*

the seal whip vibration and resulting fretting damage of the lapped sealing surfaces. The problem was finally eliminated by modifying the build procedure to eliminate a minor distortion of the outer seal plate to which the ring mates. This eliminated the low frequency vibration in the rotor response spectrum, as shown in Figure 20. The fretting damage to the lapped face was also eliminated by this build procedure.
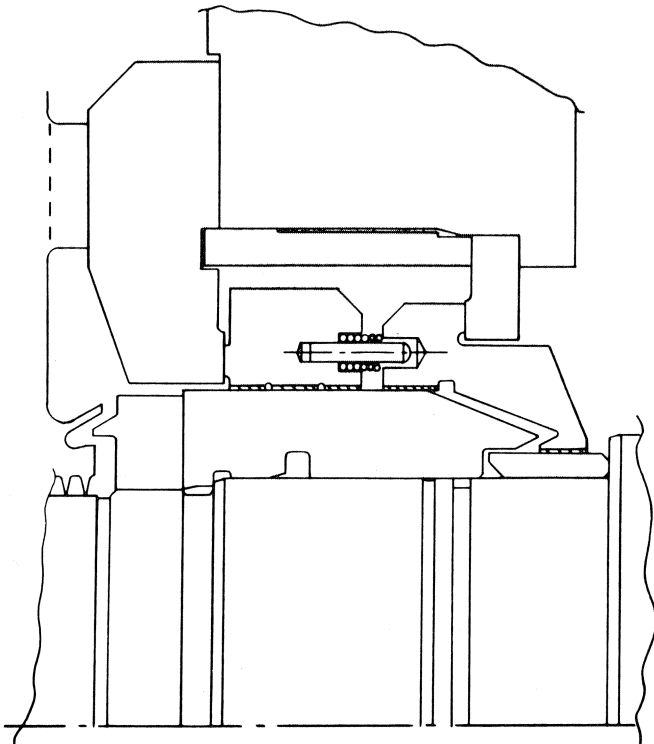

Figure 16. *Typical Cone Seal Design.*

These typical examples of oil seal instabilities were taken from low to medium pressure compressors. The behavior of the seal rings under higher pressures is of great concern and the correct calculation of seal loading and centering capacity becomes ever more critical. The experiences with past design problems and modifications to hardware, together with improved analysis capabilities will improve the chances of designing high pressure seals to optimize the compressor stability and forced response.
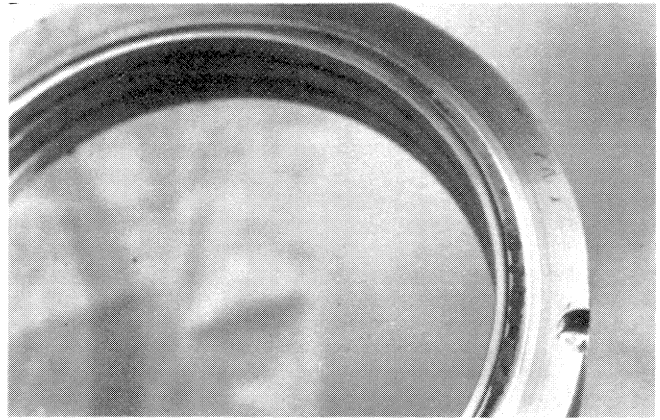

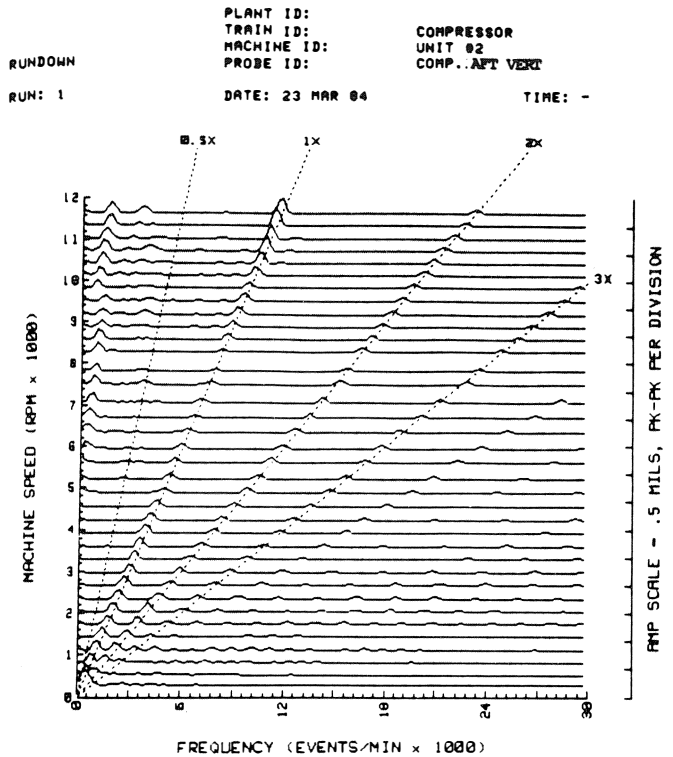Figure 17. *Outer Seal Ring Showing Fretting Damage to Lapped Sealing Face.*

Figure 18. *Vibration Resulting from Oil Ring Seal Whip.*

Recommendations for Future Research and Development

This report has documented the current analytical capability and some of the known dynamic vibration problems for oil ring seals. The analysis, while giving proper guidance, is not capable of treating the oil seal design problem in detail. Some of the areas that require further study and analysis correlation are as follows:

• Influence of seal inlet pressure distortion on seal dynamic characteristics.

• Actual pressure drop in sealing length.

• Sealing ability and pressure distribution on the lapped sealing face. Proper values are required for the parameter, β_F.

• Influence of thermal distortion on seal length.

• Actual seal running clearance as a function of seal loading.

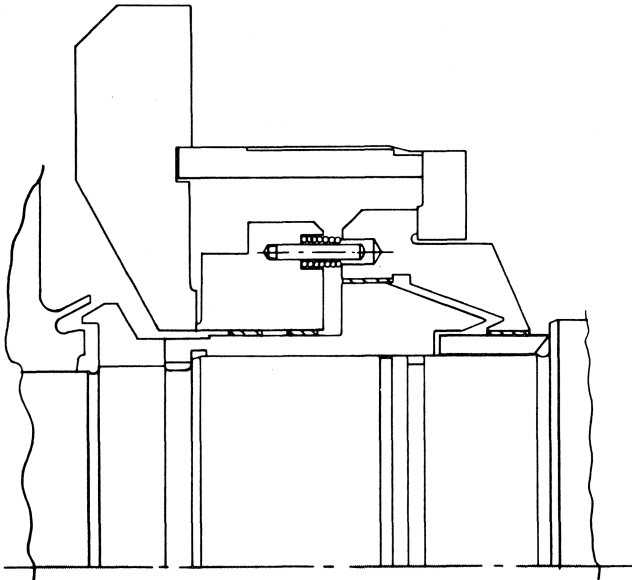• Influence of anti-rotation pin on operating eccentricity.
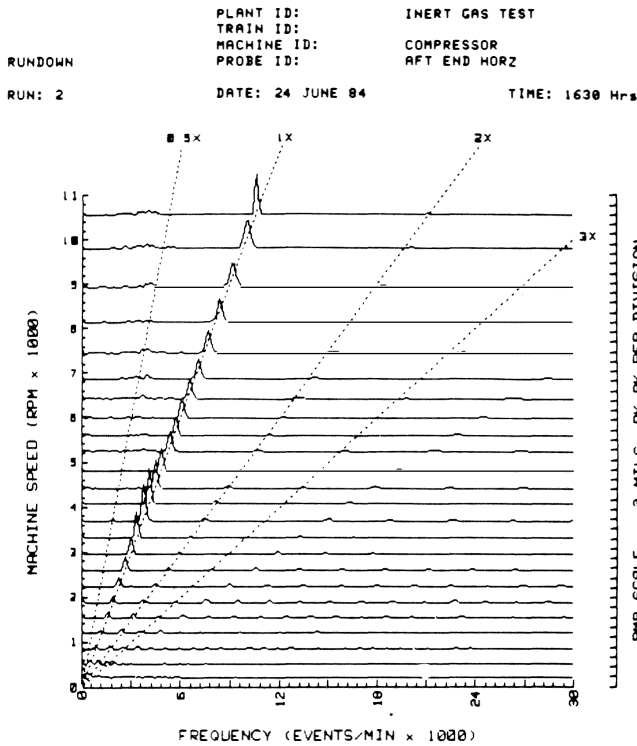
Figure 19. Pressure Balance Seal Design.

Figure 20. Rundown on Inert Gas with Modified Build Procedure Showing Absence of Oil Ring Whip.

• Influence of seal bore distortion resulting from manufacture on leakage, load capacity, and dynamic stiffness and damping.

• Benefit of added centering capacity on seal dynamic stiffness and damping.

• Influence of seal bore preload on total system design requirements.

• Influence of material types and coatings on seal lapped face fretting damage.

• Optimum pressure balance design for both response and stability.

• Research is currently in progress on many of these suggested areas and full scale testing is planned to verify and extend the analysis and design guides presented.

NOMENCLATURE

B	exponent for pressure influence on viscosity, cm^2/N
c	radial clearance, cm
$\bar{C}$	dimensionless seal damping $= \dfrac{Cc\omega}{w}$, dim
C_{xx}, C_{xy} C_{yx}, C_{yy}	bearing damping, N sec cm^{-1}
D_i	seal inside lip diameter, cm
D_o	seal outside lip diameter, cm
D_R	rotor diameter, cm
D_S	seal bore diameter, cm
E	eccentricity ratio, e/c, dim
F_{ff}	fluid film force, N
$\vec{F}_N$	axial thrust load, N
F_s	spring force, N
F_x, F_y	external seal ring loading, N
F_μ	friction load, N
h	film thickness, cm
$\bar{K}$	dimensionless seal stiffness $= \dfrac{Kc}{w}$, dim
K_{xx}, K_{xy} K_{yx}, K_{yy}	bearing stiffness, N cm^{-1}
L	active sealing length, cm
M_S	seal mass, kg
N'	rotor speed, Hz
N	rotor speed, RPM
P_o	drain pressure, N cm^{-2}
P_s	suction pressure, N cm^{-2}
ΔP	pressure drop, N cm^{-2}
R	shaft radius, cm
Re_z	axial Reynolds' number $= \dfrac{2Vc}{\nu}$, dim
Re_θ	circumferential Reynolds' number $= \dfrac{R\omega c}{\nu}$, dim
S_s	modified Sommerfeld number $=$ $\dfrac{\mu\omega LD}{2\pi W}(\dfrac{R}{c})^2(\dfrac{L}{D})^2$, rev
V	axial velocity, cm sec^{-1}
W	total seal load, N
w	seal parameter $= \dfrac{\mu\omega RL^3}{2c^2}$, N
x, y	seal relative displacement, cm
β	seal lapped face loading factor, dim
ε	eccentricity ratio, dim
θ	angle from + X-axis in direction of rotation, radians
φ	angle to line of centers from X-axis, deg
μ	oil viscosity, N sec cm^{-2}
μ_f	coefficient of friction, dim
ν	kinematic viscosity, $cm^2 sec^{-1}$
ω	rotor speed, sec^{-1}

Subscripts

i	inner seal
o	outer seal

R   rotor
S   seal
x   in x direction
y   in y direction
z   in z direction

APPENDIX

Calculation of β 2F for Assumed
Linear Lapped Face Pressure Profile

The factor $\beta 2F$ can be calculated for a linear pressure drop on the lapped face by integrating the profile pressure difference across the face width.

$$F_{pressure} = \int_{R_i}^{R_o} (P_s + \Delta P - P_o) \left[\frac{R_o - R}{R_o - R_i}\right] 2\pi R dR \qquad (A-1)$$

This results in the following expression,

$$F_{pressure} = \frac{\bar{p} \, 2\pi}{\Delta R} \left[\frac{R_o^3 - R_o R_i^2}{2} - \frac{R_o^3 - R_i^3}{3}\right] \qquad (A-2)$$

$$= \bar{p} \frac{\pi}{4} (D_o^2 - D_i^2) \beta_F$$

where

$$\bar{p} = P_s + \Delta P - P_o \qquad (A-3)$$

$$\beta_f = \frac{1 - 3\bar{D}^2 + 2\bar{D}^3}{3(1 - \bar{D})(1 - \bar{D}^2)} \qquad (A-4)$$

and

$$\bar{D} = D_i / D_o \qquad (A-5)$$

For typical value of $\bar{D}$ the following results are obtained:

Table A-1. Results of $\bar{D}$ typical values.

D_o (in)	D_i (in)	$\bar{D}$ (dim)	β (dim)
6.5	6.0	0.923	0.492
7.0	6.0	0.857	0.487
5.0	4.0	0.8	0.481

These typical results give some assurance that using an average value of $\beta_F \sim 0.5$ is a good engineering approximation for a linear pressure drop on the lapped sealing face. The operating β_F can vary due to ring distortion or end plate distortion and increase or decrease the pressure loading for given design. The actual β_F during operation is required for accurate seal operating eccentricity evaluation.

REFERENCES

1. Black, H. F., and Cochrane, E. A., "Leakage and Hybrid Bearing Properties of Serrated Seals in Centrifugal Pumps," Sixth International Conference on Fluid Sealing, Munich, West Germany (1972).

2. Black, H. F., and Jenssen, D. N., "Effect of High Pressure Ring Seals on Pump Rotor Vibrations," ASME Paper 71-WA/FE-38 (1971).

3. Kirk, R. G., and Miller, W. H., "The Influence of High Oil Seals on Turbo-Rotor Stability," ASLE Trans., *22* (1), pp. 14-24 (January 1979).

4. Kirk, R. G., and J. C. Nicholas, "Analysis of High Pressure Seals for Optimum Turbo Compressor Dynamic Performance," *Vibration in Rotating Machinery*, I. Mech. E. Proceedings of Cambridge Conference (1980).

5. Kirk, R. G., and Gunter, E. J., "Transient Journal Bearing Analysis," NASA CR-15-49, NTIS, Springfield, VA (June 1970).

6. Ocvirk, F. W., "Short Bearing Approximation for Full Journal Bearings," NACA TN 2808 (1952).

7. Wilcock, D. F., "Design of Efficient Turbulent Thrust Bearings," Trans. ASME, Journal of Lubrication Technology, ASME Paper 76-Lub-29 (1976).

8. Kirk, R. G., and Simpson, M., "Full Load Testing of an 18000 Hp Gas Turbine Driver Centrifugal Compressor for Offshore Platform Service," NASA CP-2409 (1986).

9. Fuller, D. D., *Theory and Practice of Lubrication for Engineers*, Second Edition, New York: John Wiley & Sons, pp. 51-53 (1984).